A simple stochastic model for cell population dynamics in colonic crypts

Konstantinos Mamis[a], Ruibo Zhang[a], and Ivana Bozic*[a]

[a]Department of Applied Mathematics, University of Washington, Seattle, WA 98195, USA

Abstract

Cells in colonic crypts are identified as stem, transit-amplifying (TA), or fully differentiated (FD), depending on their proliferation capability. It has been experimentally observed that the numbers of TA and FD cells vary significantly from crypt to crypt, resulting in considerable variance in the total crypt size in healthy tissue. In the present work, we propose a simple stochastic branching process to model the population dynamics of the aforementioned three cell types in a colonic crypt. We solve the model analytically, obtaining the probability distributions for the numbers of TA and FD cells, as well as the total number of cells in the crypt. For values of model parameters that correspond to healthy human crypts, all three probability distributions for TA, FD and total cell populations are in good agreement with experimental data. Furthermore, by taking into consideration the effects of *APC* and *KRAS* mutations on the number and proliferation characteristics of epithelial cells, our model is able to explain the increase in crypt size observed in early stages of colorectal tumorigenesis. Our stochastic cell population model contributes to the understanding of the mechanisms that maintain crypt size in homeostasis, and the quantification of the effects of oncogenic mutations on cell populations in the crypt.

1 Introduction

The epithelial inner surface of the human colon exhibits about 10^7 to 10^8 column-like invaginations [51], called crypts, each one of which contains about 2000 cells [50, 13]. Depending on their proliferation capability, cells in colonic crypts are identified as stem (S), transit-amplifying (TA), or fully differentiated (FD) [5, 26]. In the base of the crypt column resides a small population of about 15 stem cells [22, 41]. Stem cells divide on average once a day [22, 42, 17], producing cells that are transit-amplifying. Cell proliferation in colonic crypts is largely maintained by the TA cells, which divide every 12 to 16 hours [40, 17, 5] while they migrate upward, towards the crypt lumen. After undergoing several rounds of divisions [5, 45], they lose their proliferation capability, resulting into fully differentiated cells [37, 42]. Finally, FD cells undergo apoptosis and are shed into the intestinal lumen [24, 25]. Except for the stem cells, the total lifespan of epithelial cells, from crypt base to lumen, is 3 to 5 days [6], making thus the intestinal epithelium one of the most rapidly renewing tissues in the human body.

In order to maintain their total size, mature colonic crypts are in homeostatic steady-state, where the cell proliferation in the lower part of the crypt is in equilibrium with the FD cell loss due to apoptosis [13, 26, 25]. So far, many models have been proposed for the cell population dynamics in a crypt [46]. A large category of cell population models are spatial, and are based on the fact that the proliferation capability of each cell diminishes gradually as it moves upwards in the crypt [44, 23, 32, 47, 13]. While they can incorporate the stochasticity of cell population dynamics, the use of spatial models is based on performing simulations, since their analytic solution is intractable.

On the other hand, compartmental models for cell population dynamics that do not make use of the spatial character of cell proliferation have also been developed [35, 43, 8, 26, 19]. In this setting, the total cell population in a crypt is partitioned into different compartments, and ordinary differential equations are formulated to model the progression of cells through the compartments. The partition of cell population into compartments can be very detailed [8], can also incorporate feedback mechanisms to regulate the cell populations and maintain homeostasis [35, 26], and, in many cases, their steady-state solution is explicitly

*Corresponding author: ibozic@uw.edu

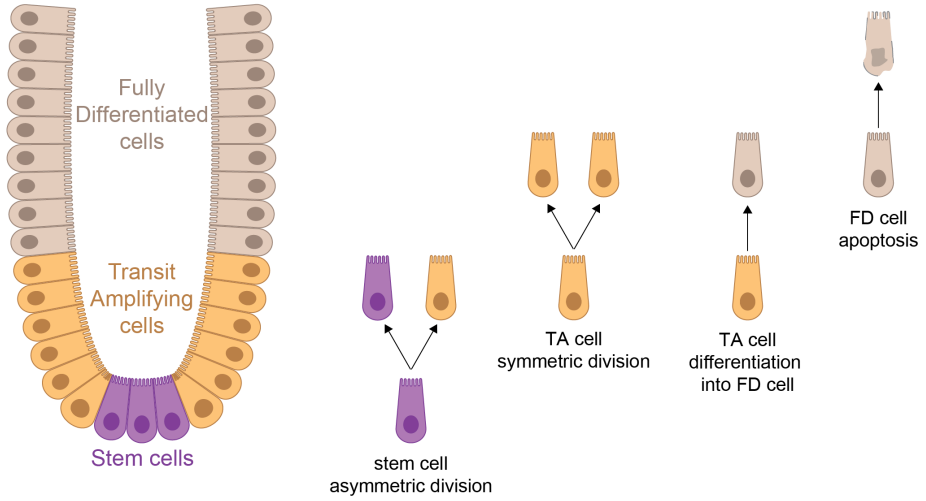

Figure 1: Schematic representation of cell populations and cell dynamics in a colonic crypt.

determined [26, 19]. However, the deterministic compartmental models cannot capture the variability in cell populations within the crypt, which is significant [44, 49, 13, 50]. Recently, stochasticity and feedback control has been incorporated in a computational compartmental model; it solution however is by numerical simulations [50].

In the present work, we propose a minimal stochastic model that **i)** is simple in its formulation, **ii)** its solution is obtained analytically, **iii)** is able to model the cell population dynamics in both healthy and mutated colonic crypts. More specifically, for healthy crypts, our model explains both the attainment of homeostatic steady-state and the variability in cell population sizes from crypt to crypt. Furthermore, our model describes the increase in size of mutant crypts [49], by considering the effects on cell properties of the most common mutations found in early stages of colorectal tumorigenesis, such as *APC* and *KRAS* [10, 4, 40].

The model we propose is the continuous-time, three-type branching process, defined by the rate equations

$$\begin{aligned} \mathrm{S} &\xrightarrow{r} \mathrm{S\ TA} \\ \mathrm{TA} &\xrightarrow{\lambda} \mathrm{TA\ TA} \\ \mathrm{TA} &\xrightarrow{d} \mathrm{FD} \\ \mathrm{FD} &\xrightarrow{\gamma} \emptyset, \end{aligned} \tag{1}$$

also depicted schematically in Fig. 1. Model (1) is stochastic, since the divisions, differentiations and apoptoses of each cell happen at random times. In model (1), the number N_0 of stem cells per crypt remains constant, since we consider that stem cells only divide asymmetrically with rate r, producing one stem and one TA cell. Recent research [39, 51] has challenged the previously held position that stem cells divide predominantly asymmetrically. Each stem cell is thought to divide symmetrically into two daughter stem cells most of the time, with asymmetry being controlled on the population level: Stemness is a property of cells residing in the stem cell niche in colonic crypt base [22, 42], and each symmetric division results in one surplus stem cell being pushed upwards, differentiating into a TA cell [31, 41]. This mechanism results in the tight regulation of stem cell numbers per crypt, which in turn allows us to assume, in our model, that stem cells *effectively* undergo asymmetric divisions, as each stem cell division ultimately results in one new TA cell. The proliferating compartment of the crypt consists mainly of the TA cell population. TA cells are rapidly-cycling, undergoing a number of cell divisions before their final differentiation [5]. In our model, TA cell behavior consists of symmetric division with rate λ, or differentiation into an FD cell with rate d. Note that cell proliferation capability depends on the location of the cell along the crypt axis, since it is controlled by signaling factors whose concentration decreases as cells move away from the crypt base [51]. Thus, in our model we assume that TA differentiations occur independently of TA divisions [30]. Last, FD cells, having lost their proliferation capability, can only undergo apoptosis with rate γ. The simplicity of the model lies in considering the minimal number of cell types in the crypt, in reflecting the upward cell migration in crypt despite not being a spatial model, and also in not considering additional homeostatic mechanisms in cell

dynamics, such as feedback control [50, 26].

Branching processes have been already used in the literature to model cell population dynamics [27], with applications in the study of mutation acquisition in cancer progression [52, 12, 11, 2], tumor progression and ctDNA shedding [3], and epidermal homeostasis [16]. In particular, epidermal homeostasis was successfully described by using an exactly solvable, two-type branching process for cell dynamics [1, 16]. Our model (1) is another example of describing a homeostatic mechanism in healthy tissue by a branching process. Note that, while branching process (1) is simple in its formulation, its solution procedure is not trivial, and its exact solution has not been derived before, to the best of our knowledge.

Our central theoretical result is the exact calculation of the joint probability generating function of TA and FD cell populations. From it, we derive explicit formulas for averages and variances of cell populations, and also calculate numerically the stationary probability distributions for TA, FD and total cell populations in a crypt.

By employing values for model parameters that correspond to healthy human crypts, we observe that the distributions from our model are in good agreement with experimental data [50, 13]. For model parameters N_0, r, λ and γ, we use typical values found in the literature on healthy human colonic crypts. Since no such direct value estimation was found for TA differentiation rate d into FD cells, we estimate d from the average crypt size observed in humans. We also consider the changes in values of model parameters, resulting from the *APC* and *KRAS* mutations that are commonly found in early stages of colorectal tumorigenesis. Under these changes, our model is able to capture the increased size and the population structure of mutant crypts.

2 Average sizes of cell populations

By considering the average change in cell population numbers per cell division or differentiation of branching process (1), we obtain a system of ordinary differential equations that describes the evolution of the average population sizes of TA and FD cells, $m_{\mathrm{TA}}(t)$, and $m_{\mathrm{FD}}(t)$ respectively:

$$\dot{m}_{\mathrm{TA}}(t) = rN_0 + (\lambda - d)m_{\mathrm{TA}}(t), \tag{2}$$

$$\dot{m}_{\mathrm{FD}}(t) = d\, m_{\mathrm{TA}}(t) - \gamma\, m_{\mathrm{FD}}(t), \tag{3}$$

where overdot denotes the derivative with respect to time t. Eqs. (2), (3) can also be derived by averaging the forward Kolmogorov equation corresponding to the branching process (1), see Supplementary Information, section S1. Under condition

$$d > \lambda, \tag{4}$$

Eqs. (2), (3) attain the steady-state solution

$$m_{\mathrm{TA}} = \frac{rN_0}{d-\lambda}, \quad m_{\mathrm{FD}} = \frac{d}{\gamma} m_{\mathrm{TA}}, \tag{5}$$

for large times, $t \to \infty$. In this setting, large times are considered those that exceed the cell cycle timescale. Steady-state solution (5) means that N_0 stem cells are able to maintain a finite, non-zero cell population in a crypt, which, on average, is equal to

$$N_{\mathrm{tot}} = N_0 + m_{\mathrm{TA}} + m_{\mathrm{FD}} = \left[1 + \frac{r}{d-\lambda} + \frac{rd}{\gamma(d-\lambda)}\right] N_0. \tag{6}$$

Also note that the steady-state solution (5) is independent from the initial populations of TA and FD cells.

We observe that violation of condition (4) results in Eqs. (2), (3) to predict an unbounded growth of both TA and FD cell numbers. Thus, stationarity condition (4) provides us with a simple mathematical description of the homeostasis for crypt size: In order for the crypt to maintain its finite size, TA cell division has to be regulated, with TA division rate λ being less than rate d of TA differentiation into FD cells. While we derived Eq. (4) for the averaged Eqs. (2), (3), it is also the stationarity condition for the stochastic population model (1).

3 Probability distribution for number of TA cells

Before solving the whole branching process (1), which results in the joint probability of TA and FD cell populations, we determine the probability distribution for the number of TA cells only. This is possible since,

in branching process (1), the number of FD cells does not affect the number of TA cells. Excluding the FD cells, and observing that asymmetric division of N_0 stem cells is equivalent to an immigration term rN_0 for TA cells, model (1) results in the one-type branching process:

$$\begin{aligned} &\emptyset \xrightarrow{rN_0} \text{TA} \\ &\text{TA} \xrightarrow{\lambda} \text{TA TA} \\ &\text{TA} \xrightarrow{d} \emptyset. \end{aligned} \tag{7}$$

For the branching process (7), we formulate and solve the corresponding evolution equation for the probability generating function (PGF) of TA cells (Supplementary Information, section S3). We see that, under condition (4), TA cell population attains stationarity, that is, for large times, the number of TA cells stays finite, and its distribution characteristics (e.g. mean and variance) remain time-invariant. The steady-state PGF for TA cell population reads

$$F_{\text{TA}}(x) = \sum_{n_1 \geq 0} P_{n_1} x^{n_1} = \left(\frac{d-\lambda}{d-\lambda x} \right)^{rN_0/\lambda}, \tag{8}$$

where P_{n_1} is the probability of having n_1 TA cells. We identify Eq. (8) as the PGF of a generalized negative binomial distribution, with the number of successes being rN_0/λ and success probability $(d-\lambda)/d$. Thus, the steady-state probability mass function for $n_1 = 0, 1, 2, \ldots$ TA cells is given by the explicit formula

$$P_{n_1} = \frac{\Gamma(n_1 + (rN_0/\lambda))}{n_1! \Gamma(rN_0/\lambda)} \left(\frac{d-\lambda}{d} \right)^{rN_0/\lambda} \left(\frac{\lambda}{d} \right)^{n_1}, \tag{9}$$

with $\Gamma(\cdot)$ being the gamma function. From Eq. (8), we calculate the average size of TA cell population for long times, which coincides with the formula in (5), and the steady-state variance of TA cell numbers:

$$\sigma^2_{\text{TA}} = \frac{rdN_0}{(d-\lambda)^2}. \tag{10}$$

4 Probability distributions for FD and total cell numbers

For branching process (1), we formulate the evolution equations for the joint probability generating function of TA and FD cell populations (Supplementary Information, section S4.1). The solution procedure for this system of equations is tedious, yet we are able to perform it analytically (Supplementary Information, section S4.2). Finally, we determine the explicit formula for the joint PGF in the long-time limit (Supplementary Information, section S4.3), which, under the stationarity condition (4), reads

$$F(x_1, x_2) = \sum_{n_1, n_2 \geq 0} P_{n_1, n_2} x_1^{n_1} x_2^{n_2} = \left(h_{-\alpha}(x_2) \frac{q_\alpha(x_2) - q_{-\alpha}(x_2)}{\alpha + 2\beta(1-x_1) + q_\alpha(x_2)} \right)^{rN_0/\lambda} \tag{11}$$

where P_{n_1,n_2} is the joint probability of having n_1 TA cells and n_2 FD cells. In Eq. (11)

$$h_{-\alpha}(x) = \Gamma(1-\alpha)(B(1-x))^{\alpha/2} I_{-\alpha}\left(2\sqrt{B(1-x)}\right), \tag{12}$$

$$q_\alpha(x) = 2\sqrt{B(1-x)} \frac{I'_\alpha\left(2\sqrt{B(1-x)}\right)}{I_\alpha\left(2\sqrt{B(1-x)}\right)}, \tag{13}$$

where $I_\alpha(x)$ is the modified Bessel function of the first kind, prime denotes the differentiation of function with respect to its argument, and the positive constants are defined as

$$\alpha = \frac{d-\lambda}{\gamma}, \quad \beta = \frac{\lambda}{\gamma}, \quad B = \frac{\lambda d}{\gamma^2}. \tag{14}$$

From Eq. (11), we calculate the steady-state average of FD population, which agrees with the respective result in Eq. (5), and the steady-state variance (Supplementary Information, section S4.5):

$$\sigma^2_{\text{FD}} = \frac{rN_0}{\lambda} \left[\frac{B}{\alpha} + \frac{B^2}{\alpha^2(\alpha+1)} \right]. \tag{15}$$

We also derive an explicit formula for the steady-state covariance of the TA and FD cell populations (Supplementary Information, section S4.6):

$$\mathsf{Cov}(\mathrm{TA}, \mathrm{FD}) = \frac{\lambda}{\gamma + d - \lambda} \sigma^2_{\mathrm{TA}}, \tag{16}$$

where σ^2_{TA} is the steady-state variance of TA cell population, defined by Eq. (10).

The marginal PGF for steady-state TA cell population is obtained from Eq. (11) for $x_2 \to 1^-$, and agrees with Eq. (8) (Supplementary Information section S4.4). Similarly, for $x_1 = 1$, Eq. (11) results in the PGF for steady-state FD cell population. From the PGFs, we are able to numerically calculate the steady-state probability mass functions of FD and total cell populations per crypt, by using Cauchy's integral formula (see Supplementary Information, section S5 for details). These distributions agree with results obtained from direct Gillespie simulations of branching process (1)(Supplementary Information, Fig. S1).

5 Comparison of model results to experimental data

For the comparison to data, we calibrate model (1) with the following parameter estimation. Values for the number N_0 of stem cells per crypt and the division rates r, λ of stem and TA cells are estimated directly from the literature; $N_0 = 15$ [22, 41], $r = 1/24\mathrm{h}^{-1}$ since stem cells divide once every day [22, 42, 17], and $\lambda = 1/14\mathrm{h}^{-1}$ since TA cells divide every 12 to 16 hours [40, 17, 5]. Also, since the total lifespan of an epithelial cell is 3 to 5 days [6], and its final differentiation occurs after the first 2 to 3 days [45], the average period from final differentiation to apoptosis is 1.5 days; thus we consider $\gamma = 1/36\mathrm{h}^{-1}$ for FD apoptosis rate. Last, we found no direct estimation in the literature for the rate d of TA cells differentiating into FD cells. We treat d as a fitting parameter for our model, so that the average total size N_{tot} of the crypt is ~ 2400 cells, matching experimental observations [50, 13]. This is performed by using Eq. (6) for average crypt size, resulting in the value $d = 0.0724\mathrm{h}^{-1}$. A similar fitting has been performed for a deterministic compartmental model for cell dynamics in hematopoiesis [19]. Despite the extensive relevant literature, precise measurements of cell populations in human colonic crypts are scarce. In the present work, we use the data of 49 crypts from human biopsy specimens conducted by Bravo and Axelrod [13, 50]. In Table 1, we compare results for average sizes and variances of TA, FD, and total cells per crypt, to the corresponding values calculated from the aforementioned data set. In Fig. 2, we show the model results for probability distributions of cell populations, along with the histograms of the experimental data, and we observe that they are in good agreement. More specifically, we find that the data are consistent with the distributions from model solution, by performing the chi-square goodness of fit test (see Supplementary Information, section S6).

The main discrepancy between our model results and data from [13] is the correlation between the TA and FD cell populations. Pearson's correlation coefficient, as calculated from data, is $\rho^{\mathrm{data}}_{\mathrm{TA,FD}} = -0.01$, while the model predicts $\rho^{\mathrm{model}}_{\mathrm{TA,FD}} = 0.97$. The observation that numbers of TA and FD cells are uncorrelated has been attributed to a feedback mechanism in cell population dynamics [50]. In our model, the correlation between

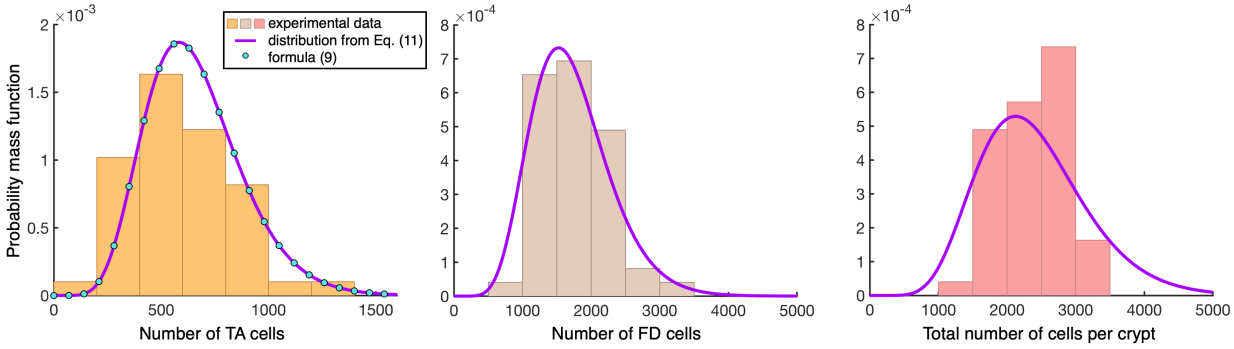

Figure 2: Steady-state probability mass function of TA, FD, and total cell populations in healthy human colonic crypts. Histograms represent experimental data [13]. Purple curves are distributions predicted by the model, calculated from the probability generating function (11) by numerical implementations of Cauchy integral formula. For TA cells, we also have the explicit distribution formula (9), denoted by circles in the first panel.

Table 1: Comparison of sizes of cell populations in healthy human colonic crypts from model and experimental data.

Cell type	Average	Variance	CV%*
TA cells (data)	608.9	$5.5 \cdot 10^4$	38.4
TA cells (model)	659.3	$5 \cdot 10^4$	34
FD cells (data)	1768.2	$1.9 \cdot 10^5$	24.6
FD cells (model)	1717.8	$3.3 \cdot 10^5$	33.3
total number of cells (data)	2392.1	$2.4 \cdot 10^5$	20.5
total number of cells (model)	2392.1	$6.3 \cdot 10^5$	33.2

*Coefficient of variation (CV%) is the ratio of the standard deviation to average, expressed as percentage.

TA and FD cell populations can be reduced significantly if we allow apoptosis rate γ to vary randomly from crypt to crypt. More specifically, by considering FD cell lifespan in each crypt to follow a continuous uniform distribution between 12 and 60h (thus having an average of 1.5 days), while keeping the average crypt size constant, correlation coefficient is reduced to $\rho_{\mathrm{TA,FD}} = 0.37$, while the cell population distributions stay close to the experimental data (see Supplementary Information, Fig. S2).

On the other hand, the proportional growth between total crypt size and the proliferative cell compartment has been experimentally observed [7], and has also been incorporated in spatial crypt models [44]. This experimental result is in agreement with the positive linear dependence between TA and total cell population in our model.

The reason for such potentially conflicting experimental results could possibly be the identification of proliferating cells as the cells that are Ki67 positively staining [13]; Ki67 staining is not a perfect differentiator between TA and FD cells, since some TA cells may not be stained due to the cell-cycle phase they currently are, and thus counted as FD cells [33]. To resolve any ambiguity, more experimental studies with larger data samples are needed for the precise quantification of the cell population sizes, variances, and their correlation.

Maintaining homeostasis under different apoptosis rates. Apoptosis rate γ is the parameter with the greatest uncertainty in the model; estimations for FD cell lifespan vary from less than a day up to 3 days. Our model is able to efficiently attain homeostasis for different FD apoptosis rates γ by adjusting TA differentiation rate d. To show this, we consider different values for γ, and for each one of these we adjust d so that the average crypt size stays ~ 2400 cells. We see in Fig. 3 that this adjustment in d results not only in keeping the average crypt sizes constant, but also leaves the crypt size distribution effectively unaltered. This is achieved by the simultaneous adjustment of the distributions for TA and FD cells: An increase in apoptosis rate γ results in an increase in the average size and variance of TA cell population and a simultaneous decrease in the FD cell population, while a decrease in γ has the opposite results. These changes in TA and FD cell populations are in agreement with the remark [36] that a large TA cell population is needed when cell turnover is high, i.e. for increased apoptosis rates γ; if γ is low, the tissue could in

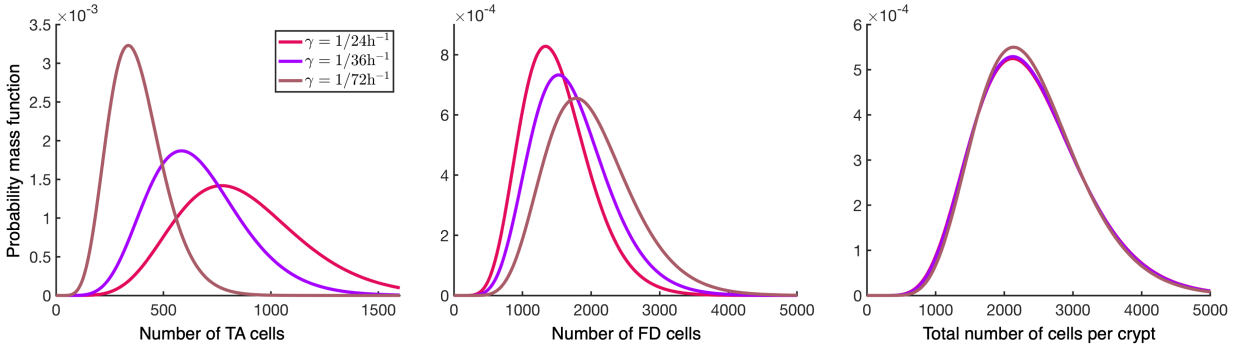

Figure 3: Steady-state probability mass function of TA, FD, and total cell populations in colonic crypts, for different apoptosis rates γ. Values for parameters N_0, r, λ are the same as in Fig. 2, and d is adjusted to keep the average crypt size constant.

principle be maintained with just stem and FD cells.

6 Effects of driver mutations on population dynamics

Having described the steady-state of healthy colonic crypts, we now use model (1) to determine the size and composition of mutated crypts in early stages of colorectal tumorigenesis, i.e. after the acquisition of certain genetic driver mutations such as *APC* and *KRAS*. *APC* inactivating mutation is sufficient for the initiation of early colorectal adenomas [29], and is present in $\sim 80\%$ of human colorectal cancers [48], resulting in the increase in proliferating cell compartment and the total crypt size [20, 9]. *KRAS* activation [34] is present in $\sim 40\%$ of human colorectal cancers and large adenomas [21], while it is often detected in human hyperplastic polyps [15]. Despite the structural alterations, mutated crypts retain the cell hierarchy described for healthy crypts [4, 40, 5].

The main effect of *Kras* mutation is the increase in division rate of stem cells to $r = 1/15\text{h}^{-1}$ [40], while the number of stem cells per crypt remains unaffected [21]. This represents a 60% increase in r compared to wild-type crypts, which divide on average once per day. This increase in stem cell division rate translates to a 60% increase in TA and FD cell populations in our model, and thus a $\sim 60\%$ increase in total crypt size. This prediction is close to the $\sim 65\%$ increase in crypt area observed experimentally [49] for human hyperplastic polyps, and the $\sim 80\%$ increase in the number of proliferating cells per crypt reported [21] in *Kras*-mutant crypts.

APC inactivation has been shown to result in the overpopulation of stem cells in the crypt [53, 4, 28, 8], without an increase in the stem cell division rate [14, 28]. By employing measurements from experiments and a model for stem cell dynamics, it has been inferred that crypts with *APC* inactivation have, on average, 1.6 times more stem cells compared to wild type crypts [4, 28]. Thus, for crypts with *APC* inactivation, we consider 24 stem cells. In our model, the average numbers of TA, FD and total cells per crypt are proportional to the number of stem cells, and thus a 60% increase in stem cell numbers results in 60% increase in the size of TA and FD cell compartments, as well as the total number of cells in a crypt. Experimentally, a proportional increase up to 100% has been observed in both the TA compartment size and total crypt size as a result of APC inactivation [38].

Last, it has been experimentally observed [49] that the difference in the average number of mitoses per area between healthy human crypts and crypts from hyperplastic polyps and adenomas is not significant. Non-elevated mitotic index has also been reported for *Apc*-deficient crypts [38]. The average number of mitoses per area is expressed equivalently as the average ratio of proliferating cells to total number of cells, which, in our model, is approximated by $m_{\text{TA}}/N_{\text{tot}} \approx m_{\text{TA}}/(m_{\text{TA}} + m_{\text{FD}}) = \gamma/(d+\gamma)$. Since the values for d and γ remain unchanged, our model predicts the same number of mitoses per area for both healthy and mutant crypts, being thus in agreement with the experimental results.

7 Discussion

In this work, we present a multitype branching process to model cell populations dynamics in colonic crypts. The simplicity in model formulation, along with its analytically obtained exact solution, provides insight of how both healthy and mutant colonic crypts maintain their size. While the solution procedure is not trivial, the model's steady-state solution is tractable, and is easily used for estimations of cell populations in colonic crypts.

For our model calibration, the only parameter fitting performed is for TA differentiation rate d; the rest of parameter values are estimated directly from the relevant literature. More specifically, we estimate d so that the average crypt size predicted by our model coincides with the experimental data. It is noteworthy that this fitting based only on average crypt size results in the predicted probability distributions for TA, FD and total cell populations to agree with experimental data.

Furthermore, the model's stationarity condition is simple, $d > \lambda$, and can also be interpreted as a criterion for malignancy in the process of colorectal carcinogenesis; model predicts unbounded growth in cell numbers when the acquired mutations result in unregulated divisions of TA cells, with division rate λ exceeding their differentiation rate d. Of course, the validation of this argument requires additional experimental evidence from late stage adenomas.

The main limitation of the model is that it presupposes the existence of homeostatic mechanisms responsible for maintaining the number of stem cells in the crypt [40, 31, 41]; thus, it is not an adequate model for

crypt cell dynamics under changes in stem cell population, such as the replenishment of their numbers after an acute stem cell loss. It has been observed experimentally [18, 17] that stem cell homeostasis is based on feedback mechanisms, such as the plasticity of early TA cells to obtain stemness again if needed. However, a crypt cell population model that incorporates these mechanisms would be more complex, and it is unlikely that its solution would be analytically tractable. Thus, such a model is outside of the scope of the present work.

Another limitation of our model is the assumption that the number N_0 of stem cells is the same in all crypts. Variation in stem cell number is reported as ± 2 cells around its average [41]. We compare our model results with constant $N_0 = 15$ for all crypts, to results where N_0 is allowed to randomly vary from crypt to crypt, with $N_0 = 13 - 17$. The averaged cell population distributions for varying N_0 coincide with the respective distributions for constant N_0 (see Supplementary Information, Fig. S3).

In summary, the usefulness of our proposed model lies in the fact that it is simple and exactly solvable, yet its results agree with experimental data; thus, it can be employed for the description and analysis of cell population dynamics in colonic crypts, without the need for computationally intensive simulations.

Data availability: The code and data used to generate the figures of the main paper and Supplementary Information can be downloaded from GitHub at https://github.com/kmamis/stochastic_model_colonic_crypts

Author contributions: K.M. and I.B. designed research; K.M., R.Z. and I.B. performed research; K.M. and I.B. wrote the paper.

Conflict of interest: The authors declare no conflict of interest.

Acknowledgements: This work is supported by the National Science Foundation grant DMS-2045166.

References

[1] T. Antal and P. L. Krapivsky. Exact solution of a two-type branching process: Clone size distribution in cell division kinetics. *Journal of Statistical Mechanics: Theory and Experiment*, 2010(7):P07028, 2010.

[2] T. Antal and P. L. Krapivsky. Exact solution of a two-type branching process: Models of tumor progression. *Journal of Statistical Mechanics: Theory and Experiment*, 2011(8):P08018, 2011.

[3] S. Avanzini, D. M. Kurtz, J. J. Chabon, E. J. Moding, S. S. Hori, S. S. Gambhir, A. A. Alizadeh, M. Diehn, and J. G. Reiter. A mathematical model of ctDNA shedding predicts tumor detection size. *Sci. Adv*, 6:eabc4308, 2020.

[4] A. M. Baker, B. Cereser, S. Melton, A. G. Fletcher, M. Rodriguez-Justo, P. J. Tadrous, A. Humphries, G. Elia, S. A.C. McDonald, N. A. Wright, B. D. Simons, M. Jansen, and T. A. Graham. Quantification of crypt and stem cell evolution in the normal and neoplastic human colon. *Cell Reports*, 8(4):940–947, 2014.

[5] N. Barker, R. A. Ridgway, J. H. Van Es, M. Van De Wetering, H. Begthel, M. Van Den Born, E. Danenberg, A. R. Clarke, O. J. Sansom, and H. Clevers. Crypt stem cells as the cells-of-origin of intestinal cancer. *Nature*, 457(7229):608–611, 2009.

[6] J. Beumer, H. Gehart, and H. Clevers. Enteroendocrine Dynamics - New Tools Reveal Hormonal Plasticity in the Gut. *Endocrine Reviews*, 41(5):1–12, 2020.

[7] M. Bjerknes and H. Cheng. The Stem-Cell Zone of the Small Intestinal Epithelium. IV. Effects of Resecting 30% of the Small Intestine. *The American Journal of Anatomy*, 160:93–103, 1981.

[8] B. M. Boman, J. Z. Fields, O. Bonham-Carter, and O. A. Runquist. Computer Modeling Implicates Stem Cell Overproduction in Colon Cancer Initiation. *Cancer Research*, 61:8408–8411, 2001.

[9] B. M. Boman, R. Walters, J. Z. Fields, A. J. Kovatich, T. Zhang, G. A. Isenberg, S. D. Goldstein, and J. P. Palazzo. Colonic Crypt Changes during Adenoma Development in Familial Adenomatous Polyposis. Immunohistochemical Evidence for Expansion of the Crypt Base Cell Population. *Am J Pathol*, 165(5):1489–1498, 2004.

[10] I. Bozic. Quantification of the Selective Advantage of Driver Mutations Is Dependent on the Underlying Model and Stage of Tumor Evolution. *Cancer Research*, 82(1):21–24, 2022.

[11] I. Bozic, T. Antal, H. Ohtsuki, H. Carter, D. Kim, S. Chen, R. Karchin, K. W. Kinzler, B. Vogelstein, and M. A. Nowak. Accumulation of driver and passenger mutations during tumor progression. *Proceedings of the National Academy of Sciences*, 107(43):18545–18550, 2010.

[12] I. Bozic and C. J. Wu. Delineating the evolutionary dynamics of cancer from theory to reality. *Nature cancer*, 1(6):580–588, 2020.

[13] R. Bravo and D. E. Axelrod. A calibrated agent-based computer model of stochastic cell dynamics in normal human colon crypts useful for in silico experiments. *Theoretical Biology and Medical Modelling*, 10(1):66, 2013.

[14] M. Bruschi, L. Garnier, E. Cleroux, A. Giordano, M. Dumas, A. F. Bardet, T. Kergrohen, S. Quesada, P. Cesses, M. Weber, F. Gerbe, and P. Jay. Loss of Apc rapidly impairs DNA methylation programs and cell fate decisions in Lgr5+ intestinal stem cells. *Cancer Research*, 80(11):2101–2113, 2020.

[15] T. L. Chan, W. Zhao, S. Y. Leung, and S. T. Yuen. BRAF and KRAS Mutations in Colorectal Hyperplastic Polyps and Serrated Adenomas. *Cancer Research*, 63:4878–4881, 2003.

[16] E. Clayton, D. P. Doupé, A. M. Klein, D. J. Winton, B. D. Simons, and P. H. Jones. A single type of progenitor cell maintains normal epidermis. *Nature*, 446(7132):185–189, 2007.

[17] H. Clevers. The intestinal crypt, a prototype stem cell compartment. *Cell*, 154(2):274–284, 2013.

[18] H. Clevers, K. M. Loh, and R. Nusse. An integral program for tissue renewal and regeneration: Wnt signaling and stem cell control. *Science*, 346(6205), 2014.

[19] D. Dingli, A. Traulsen, and J. M. Pacheco. Compartmental architecture and dynamics of hematopoiesis. *PLoS ONE*, 2(4):e345, 2007.

[20] L. E. Dow, K. P. O'Rourke, J. Simon, D. F. Tschaharganeh, J. H. Van Es, H. Clevers, and S. W. Lowe. Apc Restoration Promotes Cellular Differentiation and Reestablishes Crypt Homeostasis in Colorectal Cancer. *Cell*, 161(7):1539–1552, 2015.

[21] Y. Feng, G. T. Bommer, J. Zhao, M. Green, E. Sands, Y. Zhai, K. Brown, A. Burberry, K. R. Cho, and E. R. Fearon. Mutant kras promotes hyperplasia and alters differentiation in the colon epithelium but does not expand the presumptive stem cell pool. *Gastroenterology*, 141(3):1003–1013, 2011.

[22] H. Gehart and H. Clevers. Tales from the crypt: new insights into intestinal stem cells. *Nature Reviews Gastroenterology and Hepatology*, 16(1):19–34, 2019.

[23] T. G. Gerike, U. Paulus, C. S. Potten, and M. Loeffler. A dynamic model of proliferation and differentiation in the intestinal crypt based on a hypothetical intraepithelial growth factor. *Cell Proliferation*, 31(2):93–110, 1998.

[24] R. H. Giles, J. H. Van Es, and H. Clevers. Caught up in a Wnt storm: Wnt signaling in cancer. *Biochimica et Biophysica Acta - Reviews on Cancer*, 1653(1):1–24, 2003.

[25] P. A. Hall, P. J. Coates, B. Ansari, and D. Hopwood. Regulation of cell number in the mammalian gastrointestinal tract: the importance of apoptosis. *Journal of Cell Science*, 107:3569–3577, 1994.

[26] M. D. Johnston, C. M. Edwards, W. F. Bodmer, P. K. Maini, and S. J. Chapman. Mathematical modeling of cell population dynamics in the colonic crypt and in colorectal cancer. *Proceedings of the National Academy of Sciences*, 104(10):4008–4013, 2007.

[27] M. Kimmel and D. E. Axelrod. *Branching Processes in Biology*. Springer, New York Berlin Heidelberg, 2002.

[28] S. Kozar, E. Morrissey, A. M. Nicholson, M. van der Heijden, H. I. Zecchini, R. Kemp, S. Tavaré, L. Vermeulen, and D. J. Winton. Continuous clonal labeling reveals small numbers of functional stem cells in intestinal crypts and adenomas. *Cell stem cell*, 13(5):626–633, 2013.

[29] H. Lamlum, A. Papadopoulou, M. Ilyas, A. Rowan, C. Gillet, A. Hanby, I. Talbot, W. Bodmer, and I. Tomlinson. APC mutations are sufficient for the growth of early colorectal adenomas. *Proceedings of the National Academy of Sciences*, 97(5):2225–2228, 2000.

[30] C. P. Leblond. Classification of Cell Populations on the Basis of Their Proliferative Behavior. In C. C. Congdon and P. Mori-Chavez, editors, *Control of Cell Division and the Induction of Cancer*, pages 119–150. National Cancer Institute, Bethesda, MD, 1964.

[31] C. Lopez-Garcia, A. M. Klein, B. D. Simons, and D. J. Winton. Intestinal Stem Cell Replacement Follows a Pattern of Neutral Drift. *Science*, 330:822–825, 2010.

[32] F. A. Meineke, C. S. Potten, and M. Loeffler. Cell migration and organization in the intestinal crypt using a lattice-free model. *Cell Proliferation*, 34(4):253–266, 2001.

[33] I. Miller, M. Min, C. Yang, C. Tian, S. Gookin, D. Carter, and S. L. Spencer. Ki67 is a Graded Rather than a Binary Marker of Proliferation versus Quiescence. *Cell Reports*, 24(5):1105–1112, 2018.

[34] C. Paterson, H. Clevers, and I. Bozic. Mathematical model of colorectal cancer initiation. *Proceedings of the National Academy of Sciences*, 117(34):20681–20688, 2020.

[35] U. Paulus, C. S. Potten, and M. Loeffler. A model of the control of cellular regeneration in the intestinal crypt after perturbation based solely on local stem cell regulation. *Cell Prolif*, 25:559–578, 1992.

[36] C. S. Potten and M. Loeffler. Stem cells: attributes, cycles, spirals, pitfalls and uncertainties Lessons for and from the Crypt. *Development*, 110:1001–1020, 1990.

[37] L. E. Sanman, I. W. Chen, J. M. Bieber, V. Steri, C. Trentesaux, B. Hann, O. D. Klein, L. F. Wu, and S. J. Altschuler. Transit-Amplifying Cells Coordinate Changes in Intestinal Epithelial Cell-Type Composition. *Developmental Cell*, 56(3):356–365, 2021.

[38] O. J. Sansom, V. S. Meniel, V. Muncan, T. J. Phesse, J. A. Wilkins, K. R. Reed, J. K. Vass, D. Athineos, H. Clevers, and A. R. Clarke. Myc deletion rescues Apc deficiency in the small intestine. *Nature*, 446(7136):676–679, 2007.

[39] L. Shahriyari and N. L. Komarova. Symmetric vs. asymmetric stem cell divisions: an adaptation against cancer? *PloS one*, 8(10):e76195, 2013.

[40] H. J. Snippert, A. G. Schepers, J. H. Van Es, B. D. Simons, and H. Clevers. Biased competition between Lgr5 intestinal stem cells driven by oncogenic mutation induces clonal expansion. *EMBO Reports*, 15(1):62–69, 2014.

[41] H. J. Snippert, L. G. van der Flier, T. Sato, J. H. van Es, M. van den Born, C. Kroon-Veenboer, N. Barker, A. M. Klein, J. van Rheenen, B. D. Simons, and H. Clevers. Intestinal crypt homeostasis results from neutral competition between symmetrically dividing Lgr5 stem cells. *Cell*, 143(1):134–144, 2010.

[42] M. Spit, B. K. Koo, and M. M. Maurice. Tales from the crypt: Intestinal niche signals in tissue renewal, plasticity and cancer. *Open Biology*, 8(9):180120, 2018.

[43] I. P. M. Tomlinson and W. F. Bodmer. Failure of programmed cell death and differentiation as causes of tumors: Some simple mathematical models (tumorigenesis/apoptosis). *Proceedings of the National Academy of Sciences*, 92:11130–11134, 1995.

[44] J. Totafurno, M. Bjerknes, and H. Cheng. Variation in crypt size and its influence on the analysis of epithelial cell proliferation in the intestinal crypt. *Biophysical Journal*, 54(5):845–858, 1988.

[45] L. G. Van Der Flier and H. Clevers. Stem cells, self-renewal, and differentiation in the intestinal epithelium. *Annual Review of Physiology*, 71:241–260, 2009.

[46] I. M. M. Van Leeuwen, H. M. Byrne, O. E. Jensen, and J. R. King. Crypt dynamics and colorectal cancer: advances in mathematical modelling. *Cell Prolif*, 39:157–181, 2006.

[47] I. M.M. Van Leeuwen, G. R. Mirams, A. Walter, A. Fletcher, P. Murray, J. Osborne, S. Varma, S. J. Young, J. Cooper, B. Doyle, J. Pitt-Francis, L. Momtahan, P. Pathmanathan, J. P. Whiteley, S. J. Chapman, D. J. Gavaghan, O. E. Jensen, J. R. King, P. K. Maini, S. L. Waters, and H. M. Byrne. An integrative computational model for intestinal tissue renewal. *Cell Proliferation*, 42(5):617–636, 2009.

[48] S. M. van Neerven, N. E. de Groot, L. E. Nijman, B. P. Scicluna, M. S. van Driel, Ma. C. Lecca, D. O. Warmerdam, V. Kakkar, L. F. Moreno, F. A. Vieira Braga, D. R. Sanches, P. Ramesh, S. ten Hoorn, A. S. Aelvoet, M. F. van Boxel, L. Koens, P. M. Krawczyk, J. Koster, E. Dekker, J. P. Medema, D. J. Winton, M. F. Bijlsma, E. Morrissey, N. Léveillé, and L. Vermeulen. Apc-mutant cells act as supercompetitors in intestinal tumour initiation. *Nature*, 594(7863):436–441, 2021.

[49] W. M. Wong, N. Mandir, R. A. Goodlad, B. C.Y. Wong, S. B. Garcia, S. K. Lam, and N. A. Wright. Histogenesis of human colorectal adenomas and hyperplastic polyps: The role of cell proliferation and crypt fission. *Gut*, 50(2):212–217, 2002.

[50] J. Yang, D. E. Axelrod, and N. L. Komarova. Determining the control networks regulating stem cell lineages in colonic crypts. *Journal of Theoretical Biology*, 429:190–203, 2017.

[51] S. S. Zeki, T. A. Graham, and N. A. Wright. Stem cells and their implications for colorectal cancer. *Nature Reviews Gastroenterology and Hepatology*, 8(2):90–100, 2011.

[52] R. Zhang, O. A. Ukogu, and I. Bozic. Waiting times in a branching process model of colorectal cancer initiation. *bioRxiv*, 2022.06.22.497226, 2022.

[53] T. Zhang, K. Ahn, B. Emerick, S. R. Modarai, L. M. Opdenaker, J. Palazzo, G. Schleiniger, J. Z. Fields, and B. M. Boman. APC mutations in human colon lead to decreased neuroendocrine maturation of ALDH+ stem cells that alters GLP-2 and SST feedback signaling: Clue to a link between WNT and retinoic acid signalling in colon cancer development. *PLoS ONE*, 15(10):e0239601, 2020.